Plasmonics (2024) 19:2071–2076
https://doi.org/10.1007/s11468-023-02147-7

RESEARCH

# Cherenkov Terahertz Surface Plasmon Generation Over Graphene Surface by an Electron Beam

**Rohit Kumar Srivastav**[1]

Received: 6 November 2023 / Accepted: 26 November 2023 / Published online: 2 December 2023


## Abstract

Cherenkov terahertz (THz) surface plasmons (SPs) generation by a relativistic electron beam over the graphene surface, deposited on a $SiO_2$ substrate, is investigated. The relativistic electron beam tassel produced by SPs produces perturbed linear current density and develops THz SPs via Cherenkov interaction. Electron beam energy from 498.91 to 499.03 KeV is essential for the excitation of THz SPs of 3 to 10 THz. The growth rate of THz SPs depends on the electron beam density and Fermi energy of the graphene surface. The current investigation possesses the potential to be harnessed for the utilization of THz sensors and detectors.

**Keywords** Graphene · Terahertz · Surface plasmon · Electron beam · Fermi energy

## Introduction

In recent times, significant progress in the field of graphene research has presented novel prospects for the development of THz sources. Graphene exhibits exceptional electronic and optical properties [1]. Numerous potential applications of graphene have been successfully demonstrated [2–4]. Nevertheless, the application of this technology in generating THz radiation sources remains insufficient. There is no doubt that both theoretical and experimental research have shown that the graphene sheet has the amazing ability to keep surface plasmons (SPs) moving in the frequency range between THz and mid-infrared [5, 6]. Graphene SPs (GSPs) demonstrate notable characteristics, including enhanced mode confinement and reduced propagation loss in comparison to SPs observed in noble metal films [7, 8]. Furthermore, adjusting the electrostatic gate voltage or adding chemical doping can modify the features of graphene SPs [9, 10].

Srivastav and Panawr [11, 12] reported THz SPs generation on rippled graphene surface by p-polarized laser beam. Kumar et al. [13] observed Smith-Purcell THz radiation generation over a metallic grating by laser-modulated electron beam. Kumar et al. [14] investigated the excitation of THz radiation in an axially modulated magnetized plasma by nonlinear mixing of two CW-lasers. Kumar and Tripathi [15] studied the Cherenkov THz radiation generation over cylindrical dielectric lined resonator by the electron beam. Srivastav and Panwar [16] discussed Cerenkov THz SPs generation by electron beam on n-Insb in the presence of an external magnetic field. By using a relativistic electron beam, Kumar and Tripathi [17] studied theoretically and numerically SPs generation on a thin plasma cylinder. In their research, Kumar et al. [18] investigated the phenomenon of Cherenkov THz SPs excitation by a relativistic electron beam. An ultrathin metal film was deposited onto a glass substrate for this excitation. Tripathi et al. [19] investigated the intricate realm of Cherenkov THz radiation generation within a waveguide adorned with a dielectric lining featuring a rippled surface. This phenomenon was achieved through the utilization of a relativistic electron beam, with the esteemed researchers disclosing the requisite beam energy to be as high as 2 MeV. Zaho et al. [20] investigated the excitation of THz SPs over a circular cylindrical graphene structure by a cyclotron electron beam and reported that the THz SPs can be tuned by the beam energy and Fermi energy of graphene. Zaho et al. [21] theoretically and numerically reported THz SPs generation on a multi-layer graphene sheet deposited on a dielectric substrate with a buffer layer. Liu and Tripathi [22] investigated how an electron beam and lasers may produce SPs over a metal surface and discovered that metal can excite SPs in the infrared frequency range.

✉ Rohit Kumar Srivastav
physicsrohit93@gmail.com

[1] Department of Physics and Materials Science and Engineering, Jaypee Institute of Information Technology, A-10, Noida 201307, Utter Pradesh, India

In the present paper, theoretically and numerically investigate Cherenkov THz SPs generation by an electron beam over a graphene surface. Cherenkov THz SPs's energy may be significantly enhanced. The beam of relativistic electron Cherenkov interaction with SPs results in an altered current charge density and gives rise to the Cherenkov THz SPs. In the "THz GSPs Growth Rate" section, the THz SPs' growth rate is formulated. Discussion and conclusion are represented in the "Discussion" and "Conclusion" sections, respectively.

## THz GSPs Growth Rate

Consider an interface between free space and graphene at $x = 0$ with $x > 0$ represents free space and $x \leq 0$ represents the graphene surface. Graphene has conductivity $\sigma_g = (ie^2E_F)(\pi\hbar^2(\omega + i\nu))$ (if $E_F \geq \hbar\omega$) [23] where $e$ is electron charge, $E_F$ is Fermi energy, $\hbar$ and $\nu$ Planck constant and collision frequency, respectively.

Let us consider THz GSPs at the interface as follows:

$$\mathbf{E}_\omega = E_0 e^{-i(\omega t - k_z z)} \begin{cases} (\hat{z} + \beta_1 \hat{x}) e^{-\alpha_1 x} & \text{for x } > 0 \\ (\hat{z} + \beta_2 \hat{x}) e^{\alpha_2 x} & \text{for x} \leq 0 \end{cases} \tag{1}$$

where $\alpha_1^2 = \left(k_z^2 - (\omega^2/c^2)\right)$, $\alpha_2^2 = \left(k_z^2 - (\omega^2/(c^2\epsilon_{eff}))\right)$, $\beta_1 = -(ik_z/\alpha_1)$, $\beta_2 = -\left(ik_z/\alpha_2\right)$, $\epsilon_{eff} = \epsilon_{SiO_2} + (i\sigma_g)/(\omega\epsilon_0)$, $\alpha_1$ and $\alpha_2$ are decaying constant, $k_z$ is propagation constant of GSPs wave in direction of $\hat{z}$.

It follows the dispersion relation as follows [24]:

$$\frac{1}{\alpha_1} + \frac{\epsilon_{SiO_2}}{\alpha_2} = \frac{\sigma_g}{i\omega\epsilon_0} \tag{2}$$

In Fig. 1, let us assume that the sheet of electron beam density $n_{0b}$ propagates parallel to the graphene surface at distance $d$ (see Fig. 1). Electron beam density has velocity $v_{0b}$ in direction $\hat{z}$ and thickness $\Delta$ with perturbed density $n_{0b} = n_{0b}^0 \Delta\delta(x - d)$ and beam current $I_b = \sqrt{\pi} n_{0b}^0 \Delta b e v_b$ [18], where $b$ denotes the beam width in $\hat{y}$ direction.

Cherenkov interaction condition for electron beams and GSPs needs $\omega = k_z v_{0b}$ and gives the relationship as

$$\frac{1}{\sqrt{\frac{c^2}{v_{ob}^2 - \epsilon_{eff}}}} + \frac{\epsilon_{eff}}{\sqrt{\frac{c^2}{v_{ob}^2 - 1}}} = \frac{c\sigma_g}{i\epsilon_0} \tag{3}$$

where $\gamma_{0b} = (1 - v_{0b}^2/c^2)^{-1/2}$.

Figure 2 represents the $\gamma_{0b}$ variation with THz frequency $\omega$ for the various values of graphene Fermi energy $E_F = 0.35$ eV, 0.40 eV and 0.45 eV. The required beam energy ($E_b = (\gamma_{0b} - 1)m_0c^2$) is higher for excitation at lower THz frequencies $\omega$. Figure 2 shows that the required $\gamma_{0b}$ is 1.97469 (beam energy 498.91 KeV) to 1.97492 (499.03 KeV) for the generation of THz frequencies 3 to 10 THz.

The interaction between an electron beam and GSPs wave can be mathematically described using the equation of motion as

$$m_e^* \left[\frac{\partial}{\partial t}(\gamma \mathbf{v}) + \mathbf{v} \cdot (\nabla \gamma \mathbf{v})\right] = -e(\mathbf{E} + \mathbf{v} \times \mathbf{B}) \tag{4}$$

Upon solving Eq. (4) with $\mathbf{v} = v_{0b}\hat{z} + \mathbf{v}_{1b}$ and subsequently linearizing the equation, we obtain the perturbed velocity of the beam

$$v_{1b}^z = \frac{e}{\gamma_{0b}^3 m_e^* i\{\omega - k_z v_{0b}\}} E_z \tag{5}$$

By employing the continuity equation $\partial n/\partial t + \nabla \cdot (n\mathbf{v}) = 0$, where $n = n_{0b} + n_1$, it is possible to derive the perturbed charge density $n_1$ as

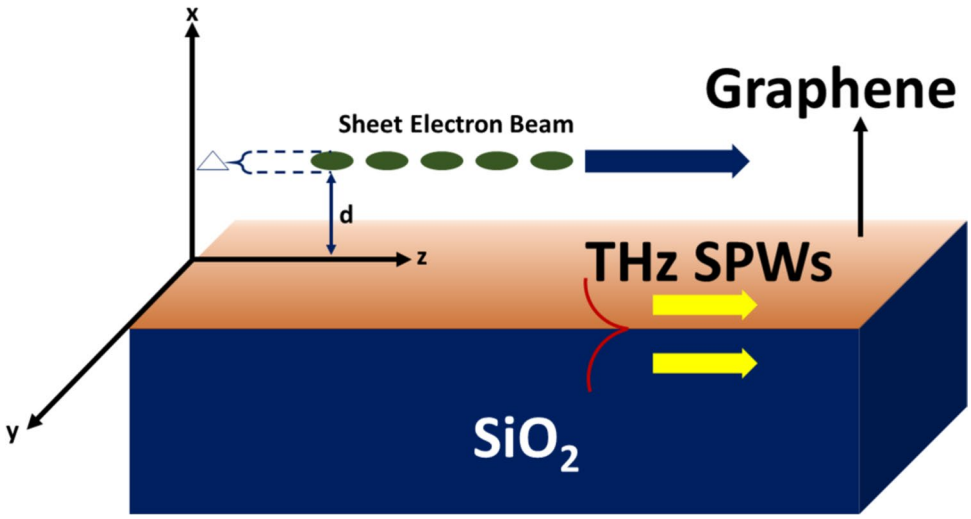


**Fig. 1** (Color Online) An electron beam with thickness Δ propagates parallel to the graphene surface at height d

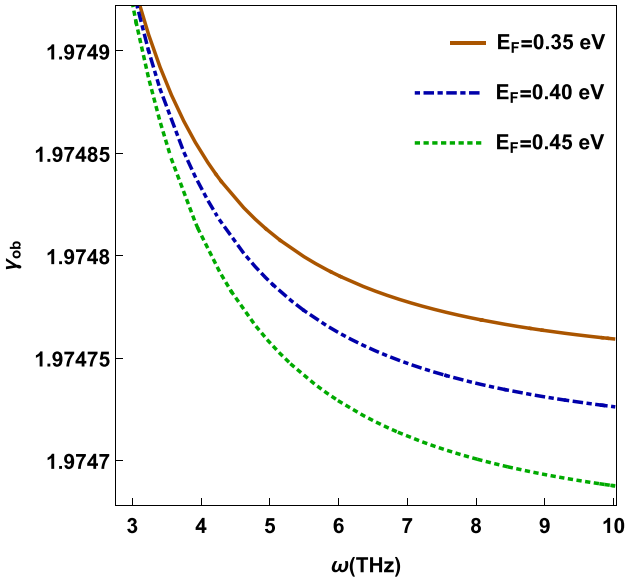


**Fig. 2** (Color Online) $\gamma_{0b}$ Vs THz frequency $\omega$ for the various values of graphene Fermi energy $E_F = 0.35$ eV (orange line), 0.40 eV (blue dot dashed line) and 0.45 eV (green dashed line)

$$n_1 = \frac{n_{0b}}{(\omega - k_z v_{0b})^2} \frac{ek_z}{m_e^* i} \frac{E_z}{\gamma_{0b}^3} \tag{6}$$

The perturbed current density $\mathbf{J}_\omega = nq\mathbf{v}$ becomes

$$J_{1,z}^{\omega} = \frac{i\triangle}{(\omega - k_z v_{0b})^2} \frac{n_{0b}^0 e^2}{m_e^*} \frac{\omega}{\gamma_{0b}^3} E_0 \delta(x-d) e^{\alpha_2 x} e^{-i(\omega t - k_z z)} \tag{7}$$

In the absence of an electron beam, the GSPs wave field mode structures are specified as $\mathbf{E}_s$ and $\mathbf{H}_s$

$$\nabla \times \mathbf{E}_s = -\mu_0 \frac{\partial \mathbf{H}_s}{\partial t} \quad \text{and} \quad \nabla \times \mathbf{H}_s = -i\omega\epsilon_0\epsilon_{eff}\mathbf{E}_s \tag{8}$$

In the presence of the perturbed beam current, the electric and magnetic fields can be expressed in terms of the electric and magnetic fields of the GSPs wave as [18, 25]

$$\mathbf{E}_b = E_1(t)\mathbf{E}_s \quad \text{and} \quad \mathbf{H}_b = E_2(t)\mathbf{H}_s \tag{9}$$

Solving Faraday's law $\nabla \times \mathbf{E}_b = -\mu_0(\partial \mathbf{H}_b/\partial t)$ and Ampere's law, $\nabla \times \mathbf{H}_b = J_{1,z}^{\omega}\hat{z} + (\partial \mathbf{D}_b/\partial t)$ with Eq. (9), we get

$$\frac{\partial E_2}{\partial t} = i\omega(E_2 - E_1) \tag{10}$$

and

$$\mathbf{E}_s \frac{\partial A_1}{\partial t} = \frac{\mathbf{J}_\omega^{nl}}{\epsilon_0\epsilon_{eff}} + i\omega(E_2 - E_1)\mathbf{E}_s \tag{11}$$

Simplify Eqs. (10) and (11) and multiply by $\mathbf{E}_s^*$, and integrating over $-\infty$ to $\infty$, we obtain

$$\frac{\partial E_1}{\partial t} = \frac{I_2}{\epsilon_0\epsilon_{eff} I_1} \tag{12}$$

where $I_1 = \int_{-\infty}^{\infty} \mathbf{E}_s \cdot \mathbf{E}_s^* dx$ and $I_2 = \int_{-\infty}^{\infty} J_{1,z}^{\omega} \cdot \mathbf{E}_{sz}^* dx$.

After solving the integrals of above equation and assuming the beam current is present $A = 1$, one may obtain

$$\frac{\partial E_1}{\partial t} = \frac{2}{\epsilon_{eff}\left(\frac{1+\beta_2^2}{\alpha_2} + \frac{1+\beta_1^2}{\alpha_1}\right)} \frac{i\triangle}{(\omega - k_z v_{0b})^2} \omega_{pb}^2 \frac{\omega}{\gamma_{0b}^3} E_1 e^{-2\alpha_1 d} \tag{13}$$

where $\omega_{pb} = (n_{0b}^0 e^2/m_e^*\epsilon_0)^{1/2}$ is plasma frequency of beam.

Let $\omega - k_z v_{0b} = i\Gamma$ and $\partial/\partial t \sim \Gamma$, we obtain,

$$\Gamma^3 = Re^{-i(\frac{2l-1}{2})\pi}$$

where

$$R = \frac{2\triangle}{\epsilon_{eff}\left(\frac{1+\beta_2^2}{\alpha_2} + \frac{1+\beta_1^2}{\alpha_1}\right)} \omega_{pb}^2 \frac{\omega}{\gamma_{0b}^3} e^{-2\alpha_1 d}$$

Or,

$$\Gamma = R^{1/3} e^{-i(\frac{2l-1}{2})\frac{\pi}{3}} \tag{14}$$

and real part of THz GSPs' growth rate ($\Gamma_r$) is given by for $l = 1$

$$\Gamma_r = \frac{\sqrt{3}}{2}\left(\frac{2\triangle}{\epsilon_{eff}\left(\frac{1+\beta_2^2}{\alpha_2} + \frac{1+\beta_1^2}{\alpha_1}\right)} \omega_{pb}^2 \frac{\omega}{\gamma_{0b}^3} e^{-2\alpha_1 d}\right)^{1/3} \tag{15}$$

THz GSPs' growth rate depends on the beam density $n_{0b}$ and Fermi energy of the graphene surface $E_F$.

The THz GSPs'efficiency [25] may be taken as

$$\eta = \frac{\Gamma_r \gamma_{0b}^3}{\omega(\gamma_{0b} - 1)} \tag{16}$$

Using the value of $\Gamma_r$ from Eq. (15) in Eq. (16), the efficiency of THz GSPs becomes

$$\eta = \frac{\sqrt{3}}{2}\left(\frac{2\triangle\omega_{pb}^2\omega}{\epsilon_{eff}\left(\frac{1+\beta_2^2}{\alpha_2} + \frac{1+\beta_1^2}{\alpha_1}\right)} e^{-2\alpha_1 d}\right)^{1/3} \frac{\gamma_{0b}^2}{\omega(\gamma_{0b} - 1)} \tag{17}$$

Equation (17) represents the efficiency of THz GSPs' growth rate and it is directly proportional to the cube root of $n_{0b}$.

The following parameters $d = 6.7 \times 10^2 \mu m$, $\Delta = 38.7 \times 10^2 \mu m$, beam density $n_{0b} = 5.72 \times 10^{16} m^{-3}$, $\gamma_{0b} = 1.97469$ (beam energy $E_b = 498.91$ KeV) and $c = 3 \times 10^8 m/sec$ are used for numerical study of THz GSPs' growth rate and efficiency in Figs. 3, 4, 5, and 6. Figures 3 and 4 represent the

variation of the ratio of THz GSPs' growth rate ($\Gamma_r^{'} = \Gamma_r/\omega$) with THz frequency $\omega$.

## Discussion

Figure 3 shows the variation of THz GSPs' growth rate $\Gamma_r^{'}$ with THz frequency $\omega$ for three values of graphene Fermi energy $E_F = 0.35$ eV, 0.40 eV, and 0.45 eV at beam energy $E_b = 498.91$. THz GSPs' growth rate exhibits a linear relationship with the THz frequency $\omega$, reaching its maximum value before declining with further increases in THz frequency. As the Fermi energy of graphene surface $E_F$ increases, the THz GSPs' growth rate peak shifts slightly toward the higher THz frequency. Also, THz GSPs' growth rate increases with decreases in Fermi energy of graphene surface $E_F$. The variation of THz GSPs' growth rate $\Gamma_r^{/}$ with THz frequency $\omega$ for the three values of beam density $n_{0b} = 5.72 \times 10^{16} m^{-3}$, $4.82 \times 10^{16} m^{-3}$, and $4.32 \times 10^{16} m^{-3}$ at Fermi energy $E_F = 0.35$ eV are plotted in Fig. 4. THz GSPs' growth rate rises as the THz frequency $\omega$ increases, reaching its maximum value before declining as the THz frequency rises further. THz GSPs' growth rate rises as beam density $n_{0b}$ rises. Figure 5 shows the THz GSPs' efficiency $\eta$ with THz frequency for various values of graphene Fermi energy $E_F = 0.35$ eV, $0.40eV$, and 0.45 eV at beam energy $E_b = 498.91$ KeV. When THz frequency $\omega$ increases, the efficiency of THz GSPs increases to a maximum and then decreases with additional THz frequency increases. THz GSPs' efficiency increases with decreases in Fermi energy of graphene surface $E_F$. Figure 6 shows the efficiency of THz GSPs' growth rate $\eta$ with THz frequency for various

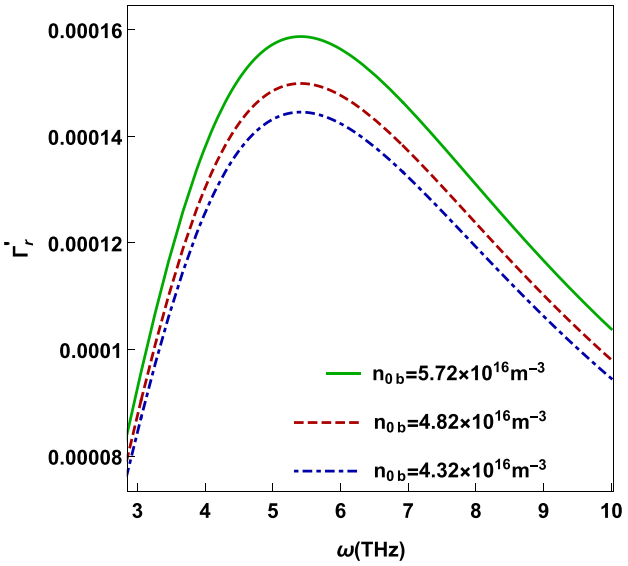


**Fig. 4** (Color Online) THz GSPs' growth rate $\Gamma_r^{'}$ Vs THz frequency $\omega$ for various values of beam density $n_{0b} = 5.72 \times 10^{16} m^{-3}$ (green line), $4.82 \times 10^{16} m^{-3}$ (red dashed line) and $4.32 \times 10^{16} m^{-3}$ (blue dot dashed line) at Fermi energy $E_F = 0.35$ eV. The other parameters are $d = 6.7 \times 10^2 \mu m$, $\Delta = 38.7 \times 10^2 \mu m$ and $c = 3 \times 10^8 m/sec$

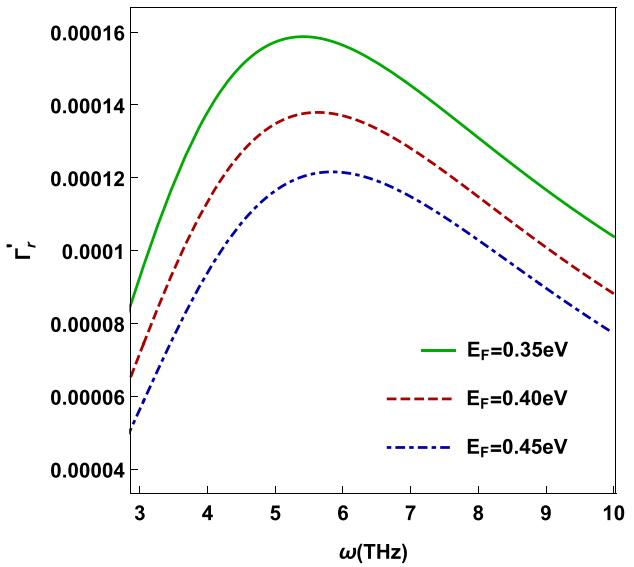


**Fig. 3** (Color Online) THz GSPs' growth rate $\Gamma_r^{'}$ Vs THz frequency $\omega$ for various values of graphene Fermi energy $E_F = 0.35$ eV (green line), 0.40 eV (red dashed line) and 0.45 eV (blue dot-dashed line) at beam energy $E_b = 498.91$ KeV. The other parameters are $d = 6.7 \times 10^2 \mu m$, $\Delta = 38.7 \times 10^2 \mu m$, beam density $n_{0b} = 5.72 \times 10^{16} \mathrm{m}^{-3}$ and $c = 3 \times 10^8 m/sec$

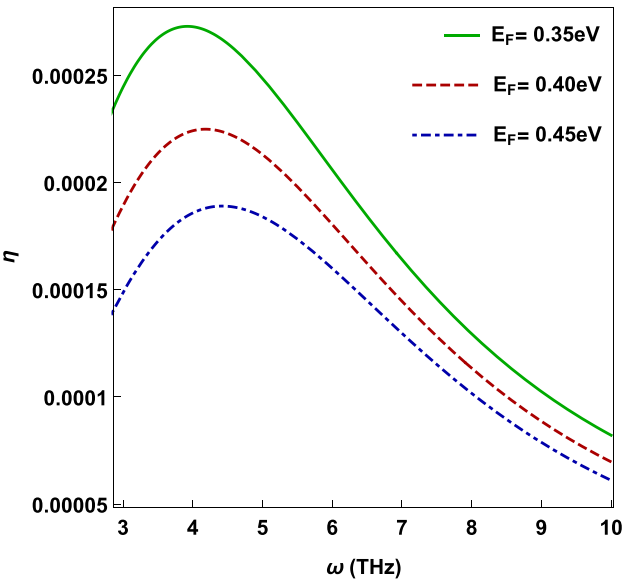


**Fig. 5** (Color Online) Efficiency of THz GSPs $\eta$ Vs THz frequency $\omega$ for various values of graphene Fermi energy $E_F = 0.35$ eV (green line), 0.40 eV (red dashed line) and 0.45 eV (blue dot-dashed line) at beam energy $E_b = 498.91$ KeV. The other parameters are $d = 6.7 \times 10^2 \mu m$, $\Delta = 38.7 \times 10^2 \mu m$, beam density $n_{0b} = 5.72 \times 10^{16} \mathrm{m}^{-3}$ and $c = 3 \times 10^8 m/sec$

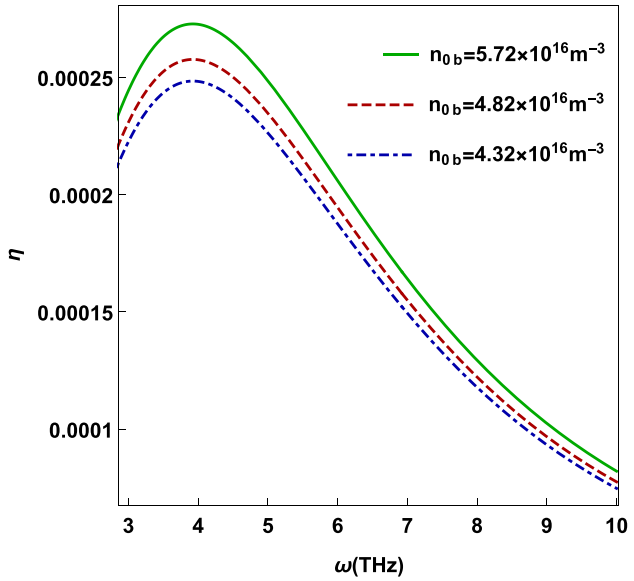


**Fig. 6** (Color Online) Efficiency of THz GSPs $\eta$ Vs THz frequency $\omega$ for various values of beam density $n_{0b} = 5.72 \times 10^{16} m^{-3}$ (green line), $4.82 \times 10^{16} m^{-3}$ (red dashed line) and $4.32 \times 10^{16} m^{-3}$ (blue dot dashed line) at Fermi energy $E_F = 0.35$ eV. The other parameters are $d = 6.7 \times 10^2 \mu m$, $\Delta = 38.7 \times 10^2 \mu m$ and $c = 3 \times 10^8 m/sec$

values of beam density $n_{0b} = 5.72 \times 10^{16} m^{-3}$ (green line), $4.82 \times 10^{16} m^{-3}$ (red dashed line), and $4.32 \times 10^{16} m^{-3}$ (blue dot dashed line) at Fermi energy $E_F = 0.35$ eV. As the normalized THz frequency increases further, the efficiency of THz GSPs decreases after reaching its maximum efficiency The efficiency of THz GSPs rises as beam density $n_{0b}$ does.

## Conclusion

In the present paper, analytically and numerically studied the THz GSPs generation by Cerenkov interaction using a relativistic electron beam over a graphene surface. The generation of THz GSPs within the frequency range of 3–10 THz necessitates an electron beam energy ranging from 498.91 to 499.03 KeV. Additionally, the Fermi energy ($E_F$) of graphene exhibits variations between 0.35 and 0.45 eV. THz GSPs' growth rate grows linearly with THz frequency for different Fermi energy of graphene, reaches its maximum value, and then drops further with a THz frequency. THz GSPs' growth rate rises with a rise in electron beam density. Kumar et al. [18] observed the maximum growth rate of THz SPs over ultra-thin metal film deposited on glass substrate approximately $10^{-6}$ by the relativistic electron beam. Sharma et al. [25] reported the efficiency of THz SPs of the order of $10^{-4}$ Here, the growth rate and efficiency of THz GSPs reported of the order of $10^{-4}$. Graphene Fermi energy, electron beam density, and electron beam energy strongly modify the growth rate and efficiency of THz GSPs. The Fermi energy of a graphene sheet may be adjusted by applying a gate voltage [26], rendering the proposed approach a dynamically adjustable device suitable for a diverse array of applications in THz graphene plasmonic and photonics devices, ultrafast switching, high-speed data transfer, and frequency conversion [27–29].

**Author Contribution** Rohit Kumar Srivastav developed the formulation of the manuscript. Rohit Kumar Srivastav prepared Figs. 1–6.

**Data Availability** The data that support the findings of this study are available from the corresponding author upon reasonable request.

## Declarations

**Ethical Approval** This declarations is "not applicable."

**Conflict of Interest** The author declares no competing interests.

## References

1. Novoselov KS, Geim AK, Morozov SV, Jiang DE, Zhang Y, Dubonos SV, Grigorieva IV, Firsov AA (2004) Electric field effect in atomically thin carbon films. Science 306:666–669
2. Liu M, Yin X, Ulin-Avila E, Geng B, Zentgraf T, Ju L, Wang F, Zhang X (2011) A graphene-based broadband optical modulator. Nature 474:64–67
3. Vakil A, Engheta N (2011) Transformation optics using graphene. Science 332:1291–1294
4. Liu S, Zhang C, Hu M, Chen X, Zhang P, Gong S, Zhao T, Zhong R (2014) Coherent and tunable terahertz radiation from graphene surface plasmon polaritons excited by an electron beam. Appl Phys Lett 104:201104
5. Ryzhii M, Ryzhii V (2007) Injection and population inversion in electrically induced p-n junction in graphene with split gates. Jpn J Appl Phys 46:L151–L153
6. Hwang E, Sarma SD (2007) Dielectric function, screening, and plasmons in two-dimensional graphene. Phys Rev B 75:205418
7. Koppens FH, Chang DE, García de Abajo FJ (2011) Graphene plasmonics: a platform for strong light-matter interactions. Nano Lett 11:3370–3377
8. Barnes WL, Dereux A, Ebbesen TW (2003) Surface plasmon subwavelength optics. Nature 424:824–830
9. Xia F, Mueller T, Lin YM, Valdes-Garcia A, Avouris P (2009) Ultrafast graphene photodetector. Nat Nanotechnol 4:839–843
10. Ju L, Geng B, Horng J, Girit C, Martin M, Hao Z, Bechtel HA, Liang X, Zettl A, Shen YR (2011) Graphene plasmonics for tunable terahertz metamaterials. Nat Nanotechnol 6:630–634
11. Srivastav RK, Panwar A (2023) Linear mode conversion of terahertz radiation into terahertz surface plasmon wave over a graphene-free space interface. Int J Mater Res 114:572–578
12. Srivastav RK, Panwar A (2023) Generation of second harmonic terahertz surface plasmon wave over a rippled graphene surface. Int J Mater Res 114:579–585
13. Kumar P, Bhasin L, Tripathi VK, Kumar A, Kumar M (2016) Smith-Purcell terahertz radiation from laser modulated electron beam over a metallic grating. Phys Plasmas 23:093301

14. Kumar M, Kang T, Kylychbekov S, Song HS, Hur MS (2021) Simulation study of phase-matched THz emission from an axially modulated magnetized plasma. Phys Plasmas 28:033101
15. Kumar M, Tripathi VK (2013) Cherenkov terahertz generation by electron bunches in a dielectric lined resonator. IEEE J Quantum Electron 49:335–339
16. Srivastav RK, Panwar A (2023) Cherenkov terahertz surface magnetoplasmons excitation by an electron beam. Phys Plasmas 30:023104
17. Kumar G, Tripathi V (2008) Excitation of a surface plasma wave over a plasma cylinder by a relativistic electron beam. Phys Plasmas 15:073504
18. Kumar P, Kumar R, Rajouria SK (2016) Cherenkov terahertz surface plasmon excitation by an electron beam over an ultrathin metal film. J Appl Phys 120:223101
19. Tripathi D, Uma R, Tripathi V (2012) Excitation of terahertz radiation by an electron beam in a dielectric lined waveguide with rippled dielectric surface. Phys Plasmas 19:093105
20. Zhao T, Gong S, Hu M, Zhong R, Liu D, Chen X, Zhang P, Wang X, Zhang C, Wu P, Liu S (2015) Coherent and tunable terahertz radiation from graphene surface plasmon polarirons excited by cyclotron electron beam. Sci Rep 5:16059
21. Zhao T, Hu M, Zhong R, Gong S, Zhang C, Liu S (2017) Cherenkov terahertz radiation from graphene surface plasmon polaritons excited by an electron beam. Appl Phys Lett 110:231102
22. Liu CS, Tripathi VK (2000) Excitation of surface plasma waves over metallic surfaces by lasers and electron beams. IEEE Trans Plasma Sci 28:353–358
23. Liu F, Qian C, Chong YD (2015) Directional excitation of graphene surface plasmons. Opt Express 23:2383–2391
24. Srivastav RK, Panwar A (2023) Linear mode conversion of terahertz radiation into terahertz surface plasmon wave over a graphene-free space interface. Int J Mater Res 114:572–578
25. Sharma SC, Malik P (2015) The effect of beam pre-bunching on the excitation of terahertz plasmons in a parallel plane guiding system. Phys Plasmas 22:043301
26. Chen J, Badioli M, Alonso-González P, Thongrattanasiri S, Huth F, Osmond J, Spasenović M, Centeno A, Pesquera A, Godignon P, Zurutuza A, Camara N, Abajo J, Hillenbrand R, Koppens F (2012) Optical nano-imaging of gate-tunable graphene plasmons. Nature 487:77–81
27. Ashish Gopal K, Singh S, Gupta DN (2023) High-intensity laser pulse interaction with a counter propagating electron beam for terahertz field generation in magnetized plasmas. Opt Quant Electron 55:605
28. Sandeep Malik HK (2023) Enhancement of Terahertz radiation due to excitation of SPW on graphene strip coated on GaAs structure. Results in Optics 13:100538
29. Bhattacharya A, Sarkar R, Kumar G (2021) Excitation of near field coupled dual toroidal resonances in a bilayer terahertz metamaterial configuration. J Phys D Appl Phys 54:285102